Articles

Influence of 1,3-Diethers on the Stereospecificity of Propene Polymerization by Supported Ziegler−Natta Catalysts. A Theoretical Investigation on Their Adsorption on (110) and (100) Lateral Cuts of $MgCl_2$ Platelets

Massimiliano Toto,[†] Giampiero Morini,[‡] Gaetano Guerra,[§] Paolo Corradini,[†] and Luigi Cavallo*,[†]

Dipartimento di Chimica, Università di Napoli, Via Mezzocannone 4, I-80134, Napoli, Italy, Montell Polyolefins, G. Natta Research Center, P.le G. Donegani 12, I-44100, Ferrara, Italy, and Dipartimento di Chimica, Università di Salerno, I-84081 Baronissi, Salerno, Italy

Received June 16, 1999; Revised Manuscript Received December 2, 1999

ABSTRACT: Energy calculations relative to the adsorption of several substituted 1,3-diethers on the unsatured (100) and (110) lateral cuts of $MgCl_2$ are presented. Independent of the particular approach used, coordination of the diethers on the (110) cut is always preferred. The energy difference favoring the diether coordination on the (110) cut depends on the substituents on carbon 2 of the 1,3-alkoxypropane skeleton. These calculated energy differences are able to rationalize the observed dependence on the chemical structure of the 1,3-diethers of the stereoregulating ability for propene polymerization of $MgCl_2$/$TiCl_4$ catalytic systems. In fact, a semiquantitative relationship has been found in the assumption that xylene-soluble (essentially atactic) and -insoluble (essentially isotactic) fractions of polypropylene obtained by these catalytic systems are prevailingly produced by Ti catalytic species adsorbed on (100) and (110) cuts, respectively.

1. Introduction

After the discovery of $MgCl_2$-supported Ziegler−Natta heterogeneous catalysts,[1] many efforts have been realized to improve their stereospecificity by using different Lewis bases.[2]

Many classes of donors have been tested during the past 20 years obtaining gradually an enhancement in terms of stereospecificity and productivity. The isotactic index, which is the weight fraction insoluble in xylene at 25 °C (w.i.), is improved from 0.4 up to 0.6 when, for example, aromatic monoesters are used as internal donors (ID), that is, mechanically treated with $MgCl_2$ and with an excess of titanium compound. Furthermore, the w.i. increases up to 0.95 if aromatic monoesters are used as both internal and external donors (ED),[3] that is, added together with the Al alkyl during the polymerization process. Moreover, w.i. increases up to 0.99 using suitable pairs of internal and external donors.[4]

Although several ID and ED have been tested, satisfactory results have been obtained with a few combinations of them only. In fact, it is well established that by using only an ID the compound is quickly removed from the surface (highly reactive toward AlR_3),[5] while the introduction in the reaction system of an ED (very stable toward AlR_3) allows to replace quickly the removed ID and is not able to displace $TiCl_4$ from $MgCl_2$.[6] Moreover, experimental data indicate that when a ED is added to the cocatalyst, not only the productivity of nonstereoregular polymer decreases monotonically[7] but also the productivity of stereoregular polymer increases up to a maximum.[8−10]

With the discovery of 1,3-diethers, it has been possible to obtain catalysts with very high performances by using only an internal donor.[11] This seems due to (a) polyfunctionality and hence scarce extraction of diethers from the solid catalytic component by the cocatalyst and (b) absence of secondary reactions with $TiCl_4$ during the catalysts preparation and with the Ti−C, Al−C, and Ti−H bonds during the polymerization.

Although the donors play a remarkable role in the Ziegler−Natta catalysis, few details are known about the mechanisms through which they interact with the other catalyst components.

Several years ago Corradini et al. have suggested that catalytic sites in relief with respect to lateral surfaces of the layered crystals are suitable to account for the similarity of the general behavior of $TiCl_3$-based and $MgCl_2$-supported catalysts.[12] In fact, magnesium dichloride has crystal structures very similar to those of violet titanium trichloride, built up of layers piled one on top of the other according to a close packing of the chlorine atoms, with the magnesium atoms occupying all the octahedral positions within each structural layer; the crystal lattice has also similar dimensions. This dictates the possibility of an epitactic coordination of $TiCl_4$ and,

[†] Università di Napoli.
[‡] G. Natta Research Center.
[§] Università di Salerno.
* Corresponding author. E-mail cavallo@chemna.dichi.unina.it.

10.1021/ma990959a CCC: $19.00
Published on Web 01/28/2000

after reduction, $TiCl_3$ units on lateral, coordinatively unsaturated, faces of $MgCl_2$ crystals, giving rise to reliefs crystallographically coherent with the matrix.

Lateral cuts of $MgCl_2$, which correspond to (100) and (110) cuts, have been observed by optical and electron microscopy on $MgCl_2$ crystal.[13] Electroneutrality conditions impose an average coordination number 5 for Mg atoms on (100) cuts and 4 for Mg atoms on (110) cuts. This causes a higher acidity of magnesium atoms on the $MgCl_2$ (110) lateral cuts, as confirmed by simple electrostatic calculations.[12] Molecular modeling studies have suggested that isolated $TiCl_3$ species formed on both lateral cuts after activation of these complexes by Al alkyl would substantially behave as nonstereospecific sites,[12] whereas the epitactic placement of Ti_2Cl_6 units on the (100) cut of $MgCl_2$ results in reliefs very similar to those proposed[14] as active sites on lateral (110) cuts of $TiCl_3$ crystals. Extensive calculations of the nonbonded interactions showed that these chiral sites can have stereoregulating ability, the main factor determining their stereospecific behavior being the fixed, chiral orientation into which the growing polymer chain appears to be forced.[12]

The low stereospecificity of $MgCl_2$-supported catalysts has been explained assuming that, upon coordination of $TiCl_4$ to $MgCl_2$, mononuclear and dinuclear species are formed (as suggested by ESR[15]) at both (100) and (110) cuts and only dinuclear species on the (100) cuts leading to the formation of stereospecific sites.[12] In this framework, it was proposed that the role of internal donors in increasing the stereospecificity of supported catalysts could be related to the ability of titanium chloride to displace the donor preferentially from the less acidic (100) cut.[7]

As for the increase of productivity of stereoregular polymer which can be observed for suitable addition of an ED, it has been proposed that the adsorption on the $MgCl_2$ (100) lateral cut would shift the equilibrium between aspecific (isolated) and stereospecific (nonisolated) centers toward the stereospecific ones.[7] Molecular mechanics calculations have suggested an additional explanation involving a direct steric effect transforming nonstereospecific sites into stereospecific ones.[11b,16]

Some studies relative to the interactions between 1,3-diethers and $MgCl_2$ supports have been already published. Iiskola et al.[17] proposed that 1,3-diethers can act as bidentate ligands on (110) $MgCl_2$ cut with magnesium atom which have two vacant coordination sites.

Scordamaglia et al. studied the chelating effect of different Lewis bases[16] and the correlation between the probability of conformations leading to O−O distances suitable for chelating coordination to tetracoordinated Mg atoms and their effect in stereoregulation in propene polymerization.[11b,18]

Although these studies have clarified some aspects relative to the interactions between these different species, a systematic theoretical investigation of the coordination of 1,3-diethers to (100) and (110) cuts of $MgCl_2$ is still missing. With this aim, we studied the adsorption of several 1,3-diethers substituted in position 2 on the (110) and (100) cuts of $MgCl_2$ by two different approaches: the computationally inexpensive molecular mechanics (MM) technique widely used in the field of Ziegler−Natta catalysis, which allows to scan a large number of systems, and a more reliable quantum mechanics approach (the semiempirical AM1 method), which offers a more quantitative analysis.

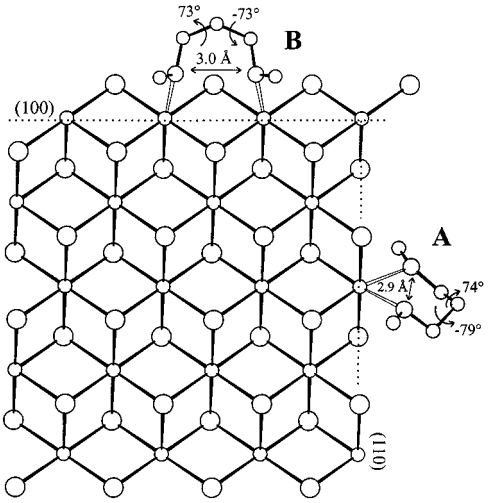

Figure 1. Schematic drawing of a $Mg_{20}Cl_{40}$ cluster. AM1 optimized geometries of 1,3-dimethoxypropane molecule adsorbed on the (110) and the (100) cuts are shown in parts A and B, respectively. Both structures correspond to an almost C_s symmetric (G^+,G^-) conformation. Only the position of 1,3-dimethoxypropane has been optimized. Hydrogen atoms of 1,3-dimethoxypropane have been omitted for clarity. Hollow bonds are used to indicate bonds between the diether and the $Mg_{20}Cl_{40}$ cluster.

2. Methods and Models

MM and AM1 analyses have been performed on $MgCl_2$ clusters with an adsorbed donor molecule. (100) and (110) cuts of a $MgCl_2$ cluster with an adsorbed donor molecule are shown in Figure 1. To simplify our analysis, the smaller Mg_6Cl_{12} and Mg_7Cl_{14} clusters (see Figures 3 and 4) have been used to represent the (110) and (100) cuts, respectively.

The Mg−Cl bond distances and the Mg−Cl−Mg angles have been set equal to 2.49 Å and 90°, respectively. This corresponds to the simplifying assumption that the atoms on the surface present a structure very close to that present in the bulk of crystal. While the geometry of the $MgCl_2$ clusters has been kept fixed in all the calculations here reported, the geometries of adsorbed donor molecules have been always fully optimized. The main dihedral angles minimized in our calculations are θ_1 and θ_2, defined as the rotation around the C_1-C_2 and C_2-C_3 bonds, respectively (see Figure 2A).

The MM calculations have been performed by using the CHARMM force field,[19] while the nonbonded parameters for Mg and Cl are those reported in the UFF force field.[20] The Mg−O bond distances have been fixed to 2.05 Å, that is, equal to Mg−O average bond distances reported in ref 21. To check the dependence of the calculations on the Mg−O distance, values in the range 2.0−2.3 Å have been tested, obtaining qualitatively similar results. As in analogous MM studies on homogeneous and heterogeneous Ziegler−Natta catalysts, for the nonbonded interactions we assumed a pure repulsive potential in according to a modified Lennard-Jones functional.[22]

The quantum-mechanics calculations have been performed with the semiempirical molecular orbital package MOPAC93.[23] The AM1 semiempirical Hamiltonian has been used.[24] With respect to the original parameters for Mg proposed by Stewart,[25] a later implementation of AM1 with Mg parameters proposed by Hutter has been considered.[26] These new Mg parameters seem able

to describe structures having heavy atoms next to magnesium better than the original Mg parameters.

To validate the AM1 analysis, test calculations using a density functional theory (DFT) approach have been performed for adsorption of 1,3-dimethoxypropane on the (110) and (100) cuts of the $Mg_{12}Cl_{24}$ and $Mg_{11}Cl_{22}$ clusters, respectively. For these tests, the ADF package developed by Baerends et al. has been used.[27] The electronic configurations of the systems were described by an uncontracted triple-ζ STO basis set on Mg (3s, 3p, 3d),[28] while a double-ζ STO basis set was used for H, C, O (2s, 2p), and Cl (3s, 3p).[28] These basis sets were augmented with a single 2p or 3d polarization function on H and on C, O, and Cl, respectively. The $1s^2 2s^2 2p^6$ configuration on Mg and Cl and the $1s^2$ configuration on C and O were treated by the frozen-core approximation. Energies and geometries have been obtained by using the local potential by Vosko et al.,[29] augmented in a self-consistent manner by the Becke's exchange gradient correction[30] and by the Perdew's correlation gradient correction.[31,32]

3. Energy Decomposition

The donor complexation energy, E, is calculated according to eq 1:

$$E = E_{Mg/D} - E^0_{Mg} - E^0_{D} \quad (1)$$

where $E_{Mg/D}$ is the total energy of the system composed by a donor molecule bonded on the Mg_nCl_{2n} cluster, while E^0_{Mg} and E^0_{D} are the total energies of the Mg_nCl_{2n} cluster and free donor, respectively. However, for analysis purposes the donor complexation energy can be rewritten according to eq 2:

$$E = E_{Intra} + E_{Inter} \quad (2)$$

where $E_{Intra} = E_D - E^0_D$ is the energy required to deform a free donor molecule in a conformation suitable to be bonded on the surface, that is, the geometry assumed in the final system. E_{Inter}, instead, describes the interaction energy between the distorted donor and the Mg_nCl_{2n} cluster. Combining eqs 1 and 2, we obtain

$$E_{Inter} = E_{Mg/D} - E^0_{Mg} - E_D$$

It is worth noting that E_{Intra} is by definition always positive, whereas E_{Inter} is positive by using the MM method and negative by using the AM1 approach. In fact, in our MM analysis only the repulsive term of the nonbonded Lennard-Jones potential has been considered in order to avoid negative contributions to the energy. This approach presents the advantage of enphasizing the "steric properties" of a molecular system and to evaluate steric repulsive interactions between the Mg_nCl_{2n} cluster and the donor molecule. On the contrary, the AM1 E_{Inter} represents the total interaction energy (mainly electrostatic) between the Mg_nCl_{2n} cluster and the donor molecule. Consequently, the MM E are always positive (steric effects can be "weighed"), whereas the AM1 E are always negative (a complexation energy for the adsorbed donor molecules is calculated).

4. Analysis and Discussion

The conformational energy minima of 1,3-dimethoxypropane are presented in Figure 2. Because of the symmetry of the diether, only four independent minima

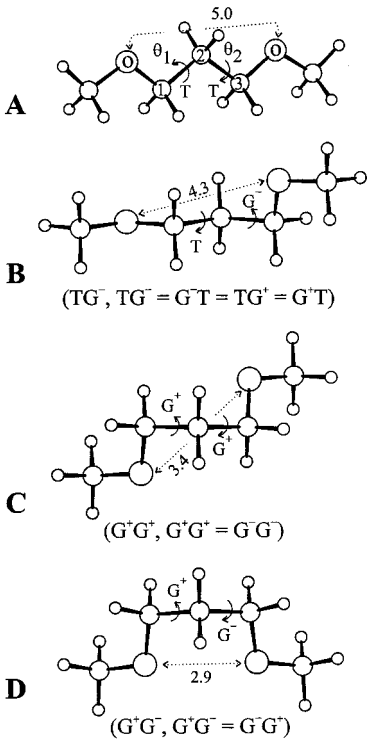

Figure 2. MM fully optimized geometries of 1,3-dimethoxypropane. Models A, B, C, and D correspond to (T,T), (T,G$^-$), (G$^+$,G$^+$), and (G$^+$,G$^-$) conformations, respectively Due to the symmetry of the diether, four equivalent minimum-energy confomations are described by model B, two equivalent minimum-energy confomations by model C, and two equivalent minimunm-energy confomations by model D.

are present corresponding to (T,T), (T,G$^-$), (G$^+$,G$^+$), and (G$^+$,G$^-$) conformations, respectively. MM analysis indicates that the (T,T) conformation represents the absolute minimum, while (T,G$^-$), (G$^+$,G$^+$), and (G$^+$,G$^-$) conformations are 0.3, 0.5, and 0.9 kcal/mol higher in energy, respectively. The AM1 approach provides substantially similar results. The (T,T) conformation is still the absolute minimum, while (T,G$^-$), (G$^+$,G$^+$), and (G$^+$,G$^-$) conformations are 0.1, 0.3, and 1.0 kcal/mol higher in energy, respectively.

It is worth noting that only the C_s symmetric (G$^+$,G$^-$) and the C_2 symmetric (G$^+$,G$^+$) conformations (and their equivalents) are particularly relevant in the framework of the present analysis, because these conformations present O−O distances suitable for bonding to the $MgCl_2$ surface. In fact, as recently suggested, the O−O distance in the high-performance 1,3-diethers are usually in the 2.8−3.2 Å range.[18] These O−O distances are optimal for the diethers−$MgCl_2$ surface interaction.[18]

The MM optimized geometries of 1,3-dimethoxypropane coordinated on the (110) and (100) lateral cuts of the $MgCl_2$ cluster are shown in Figures 3 and 4, respectively, and the corresponding values of the θ_1 and θ_2 dihedral angles and of the oxygen−oxygen distances as well as the corresponding energies are collected in Table 1.

The coordinated donor presents a pseudo chair conformation with a local almost C_s symmetry in Figure 3A, whereas the coordinated donor adopts a C_2 symmetry which perfectly fits with the local C_2 symmetry of the support in Figure 3B. Local almost C_s and C_2 symmetries are also present in the model shown in Figure 4, parts A and B, respectively. Besides, an energy

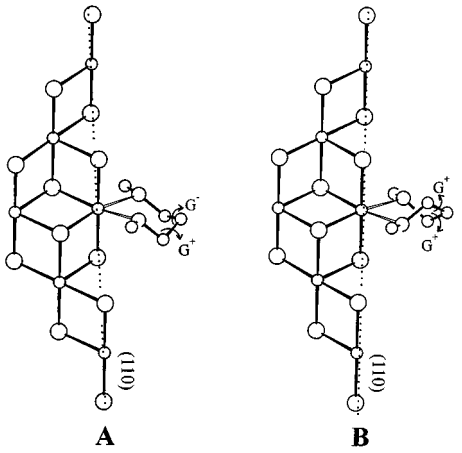

Figure 3. MM optimized geometries of 1,3-dimethoxypropane adsorbed on the (110) cut of the Mg_6Cl_{12} cluster. Only the position of 1,3-dimethoxypropane has been optimized. A corresponds to the almost C_s symmetric (G^+,G^-) conformation, while B corresponds to the C_2 symmetric (G^+,G^+) conformation. Hydrogen atoms of 1,3-dimethoxypropane have been omitted for clarity. Hollow bonds are used to indicate bonds between the diether and the Mg_6Cl_{12} cluster.

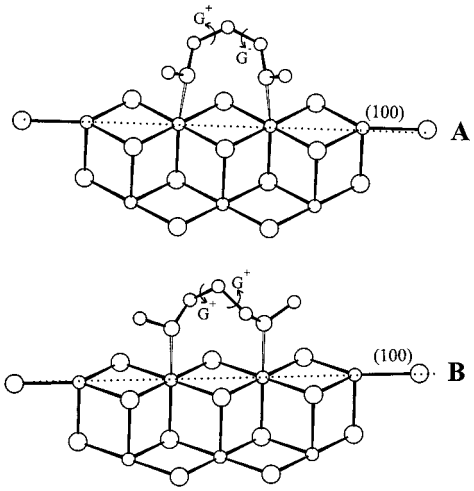

Figure 4. MM optimized geometries of 1,3-dimethoxypropane adsorbed on the (100) cut of the Mg_7Cl_{14} cluster. Only the position of 1,3-dimethoxypropane has been optimized. A and B correspond to the C_s symmetric (G^+,G^-) and C_2 symmetric (G^+,G^+) conformations, respectively. Hydrogen atoms of 1,3-dimethoxypropane have been omitted for clarity. Hollow bonds are used to indicate bonds between the diether and the Mg_7Cl_{14} cluster.

and geometric comparison between AM1 and MM optimized structures is also reported in Table 1.

The energy comparison (see Table 1) indicates that the donor molecule is preferentially coordinated on the (110) $MgCl_2$ lateral cut and that the lowest energy minimum corresponds to the (G^+,G^-) conformation. (Because of the absence of chirality of the active sites, the minimum with (G^-,G^+) is equivalent.) Moreover, this conformation presents the lowest E_{Intra} value (that is, the energy required to deform the molecule in a geometry suitable for coordination), independent of the computational approach. The AM1 E_{Inter} values for diether coordination on the (110) cut are substantially lower than the values for diether coordination on the (100) cut, indicating a better interaction of the diether with the (110) cut. The substantially similar MM E_{Inter} values between the two lateral cuts suggest that diethers coordination is not driven by repulsive interactions between the diether and the $MgCl_2$ surface. As for the donor complexation energy differences $\Delta E = (E^{(100)} - E^{(110)})$ between the (100) and (110) cuts, it strongly depends on the computational method. In fact, by the MM approach coordination on the (110) cut is favored by roughly 1 kcal/mol, whereas by the AM1 approach coordination on the (110) cut is favored by roughly 6 kcal/mol. This is due to the fact that the AM1 calculations account for binding contributions (mainly electrostatic) which are neglected in our MM approach. The larger AM1 E values indicate an intrinsic preference for coordination on the (110) cut, in agreement with the suggested more acidic behavior of the (110) cut.[12] On the other hand, the MM E values suggest a concurrent effect that favors the diether coordination on the (110) cut; in fact, a smaller energy is required to deform the free diether molecule in a conformation suitable for adsorption on the (110) cut.

To test the dependence of our results on the cluster size, AM1 calculations for coordination of 1,3-dimethoxypropane on the larger $Mg_{20}Cl_{40}$ cluster have been performed.

The minimum-energy situations corresponding to the diether adsorption on the (110) and (100) cuts correspond to the (G^+,G^-) conformation and are reported in Figure 1. The donor complexation energies, E, are −36.8 and −28.9 kcal/mol, respectively. The energies and the geometries obtained with the larger cluster are very close to the energies of the corresponding structures, which have been obtained with the smaller cluster (Table 1), supporting the validity of our model. Finally, DFT test calculations have been also carried out. E calculated for models corresponding to the adsorption of dimethoxypropane in the (G^+,G^-) conformation on (110) and (100) cuts of $Mg_{12}Cl_{24}$ and $Mg_{11}Cl_{22}$ clusters, respectively, are −33.6 and −30.7 kcal/mol, respectively. Again the diether coordination on the (110) cut is favored, and the DFT E are in a good agreement with the AM1 E.

The above-described general approach has been extended to several 1,3-diethers with the same basic

Table 1. Comparison between Geometries and Energies ($E = E_{Intra} + E_{Inter}$) for 1,3-Dimethoxypropane Coordination on the (100) and (110) Cuts of $MgCl_2$, Obtained Using the MM and AM1 Approaches

	MM				AM1			
	(110)		(100)		(110)		(100)	
	G^+G^-	G^+G^+	G^+G^-	G^+G^+	G^+G^-	G^+G^+	G^+G^-	G^+G^+
Figure	3A	3B	4A	4B	3A	3B	4A	4B
θ_1 (deg)	70	39	62	61	75	42	75	61
θ_2 (deg)	−75	38	−62	61	−80	43	−75	61
d(O−O) (Å)	2.8	2.9	2.7	3.6	2.9	2.9	3.0	3.6
E (kcal/mol)	5.9	8.0	7.0	10.1	−38.3	−37.5	−32.5	−31.1
E_{Inter} (kcal/mol)	1.8	5.3	3.2	4.6	4.7	6.1	5.9	6.9
E_{Intra} (kcal/mol)	4.1	2.7	3.8	5.5	−43.0	−43.6	−38.4	−38.0

Table 2. Donor Complexation Energies ($E^{(110)}$ and $E^{(100)}$) for Coordination of 2,2′-Substituted 1,3-Diethers of Scheme 1 on the (110) and (100) Cuts of $MgCl_2$, Respectively, and Their Differences ($\Delta E = E^{(100)} - E^{(110)}$), Using MM and AM1 Approaches

	MM			AM1			
donor	$E^{(110)}$ (kcal/mol)	$E^{(100)}$ (kcal/mol)	ΔE (kcal/mol)	$E^{(110)}$ (kcal/mol)	$E^{(100)}$ (kcal/mol)	ΔE (kcal/mol)	w.i.[33]
1	5.9	7.0	1.1	−38.3	−32.5	5.8	0.649
2	6.2	7.2	1.0	−38.7	−33.1	5.6	0.749
3	6.7	9.6	2.9	−38.4	−31.0	7.4	0.877
4	6.9	8.1	1.2	−40.2	−34.2	6.0	0.895
5	6.3	9.4	3.1	−40.2	−32.5	7.7	0.898
6	7.9	12.2	4.3	−41.9	−30.6	11.3	0.953
7	7.6	12.5	4.9	−39.6	−29.0	10.6	0.954
8	7.0	9.8	2.8	−40.1	−31.4	8.7	0.958
9	5.8	11.8	6.0	−40.9	−27.9	13.0	0.960
10	10.3	14.9	4.6	−42.5	−31.6	10.9	0.975
11	6.1	13.1	7.0	−46.4	−31.2	15.2	0.977
12	7.7	12.8	5.1	−41.1	−29.1	12.0	

Scheme 1

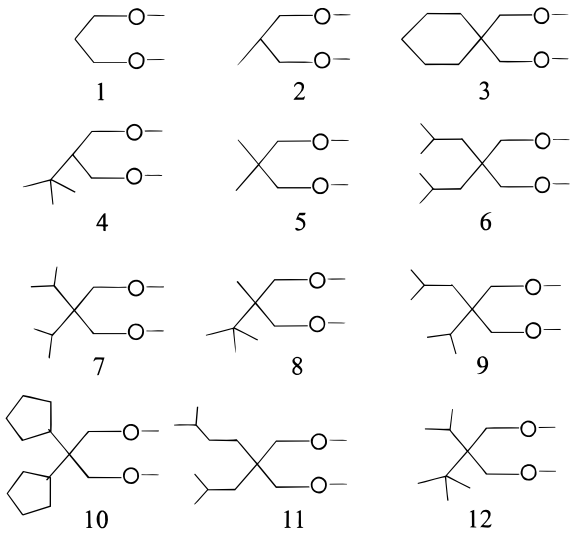

skeleton but different substituents in position 2,2′ (see Scheme 1). The calculated AM1 and MM E, for the minimum-energy (G^+,G^-) conformations, are reported in Table 2. For all the considered systems, the AM1 and MM E values for the (110) cut are lower, indicating that coordination on the (110) cut is favored.

It is interesting to note that, in plotting the AM1 ΔE versus the MM ΔE (see Figure 5), the points are quite

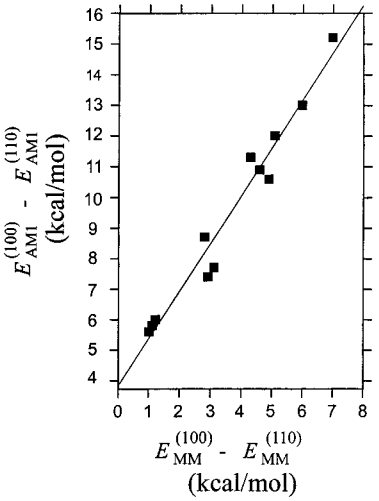

Figure 5. Energy plot of the $E^{(100)} - E^{(110)}$ AM1 values versus the $E^{(100)} - E^{(110)}$ MM values for the donors reported in Scheme 1.

Table 3. Energy Differences ($\Delta E_{Intra} = E_{Intra}^{(100)} - E_{Intra}^{(110)}$) and ($\Delta E_{Inter} = E_{Inter}^{(100)} - E_{Inter}(110)$) for Coordination of the 2,2′-Substituted 1,3-Diethers of Scheme 1 on the (110) and (100) Cuts of $MgCl_2$, Obtained Using the MM and AM1 Approaches

	MM		AM1	
donor	ΔE_{Intra} (kcal/mol)	ΔE_{Inter} (kcal/mol)	ΔE_{Intra} (kcal/mol)	ΔE_{Inter} (kcal/mol)
1	1.5	−0.4	1.2	4.6
2	1.4	−0.4	1.5	4.1
3	2.4	0.5	1.6	5.8
4	1.6	−0.4	1.5	4.5
5	2.4	0.7	1.0	6.7
6	3.5	0.8	2.6	8.7
7	3.9	1.0	2.4	8.2
8	2.1	0.7	2.0	6.7
9	4.9	1.1	2.8	10.2
10	3.7	0.9	2.6	8.3
11	5.9	1.1	2.9	12.3
12	3.9	1.2	2.9	9.1

well lined up on a straight line, indicating that for all considered donors both methods qualitatively provide almost same trends. It is also worth noting that the size of the diethers substituents has a direct influence on both MM and AM1 ΔE values. The MM ΔE values increase as the substituents size increase, because more energy is required to prepare the diether for coordination on the (100) cut (greater $\Delta E_{Intra} = E_{Intra}(100) - E_{Intra}(110)$ values, see Table 3), and the diether repulsively interacts with the $MgCl_2$ (100) cut (greater $\Delta E_{Inter} = E_{Inter}(100) - E_{Inter}(110)$ values, see Table 3). The AM1 ΔE values are more sensitive to the size of diether substituents because the reduced interactions of the more crowded donors with the (100) cut also reduces the attractive electrostatic interactions.

In the simplifying assumption that the xylene-insoluble and -soluble polymer fractions are substantially produced by fully isospecific (subscript i) and less isospecific sites (aspecific, subscript a), respectively, it can be written that

$$\frac{1 - \text{w.i.}}{\text{w.i.}} \cong \frac{k_a C_a}{k_i C_i} \tag{3}$$

where k_i, k_a and C_i, C_a are kinetic constants relative to chain propagation reaction and to surface concentration of isospecific and aspecific sites, respectively. For the purpose of a comparison between different diether donors, C_a/C_i can be written as $K \exp(-\Delta E/RT)$, where ΔE is an *apparent* difference in energy, typical of each diether donor.

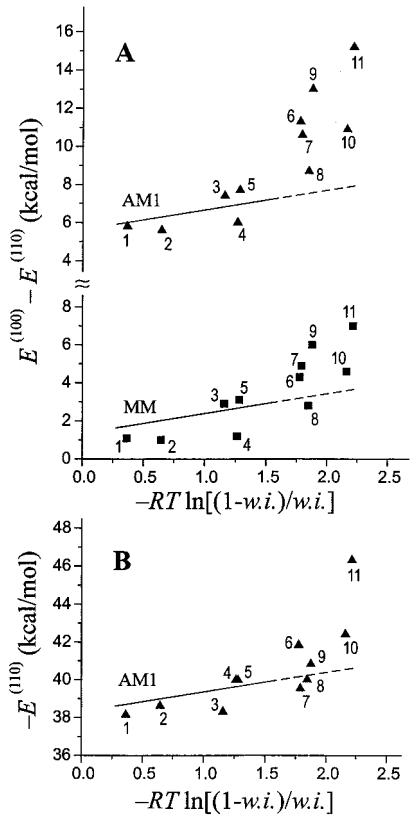

Figure 6. Energy plots of the $E^{(100)} - E^{(110)}$ values calculated by the AM1 and MM methods versus $-RT \ln[(1 - \text{w.i.})]/\text{w.i.}$), part A, and of the $-E^{(110)}$ values calculated by the AM1 method, part B. The numbers close to the plotted points refer to the numbering of the donors reported in Scheme 1.

In Figure 6, we report plots of $-RT \ln[(1 - \text{w.i.})/\text{w.i.}]$ versus the $[E^{(100)} - E^{(110)}]$ values, as calculated by the AM1 and MM methods (Figure 6A), and the $-E^{(110)}$ values, as calculated by the AM1 methods (Figure 6B). The plots are indicative of a correlation; in particular, a roughly linear correlation seems to hold at least in the range of $(1 - \text{w.i.}) > 0.1$. This range possibly corresponds not only to experimental data less affected by errors but also to more reliable calculated energies, due to smaller bulkiness of the diether substituents.

This behavior can be tentatively rationalized in the assumption that titanium compounds compete with the donor for coordination on MgCl$_2$ lateral cuts, leading to a *full coverage* of the MgCl$_2$ lateral cuts, and that isospecific and aspecific Ti sites are formed on the (100) and (110) MgCl$_2$ lateral cuts, respectively.

Under these assumptions it can be written that

$$\frac{1 - \text{w.i.}}{\text{w.i.}} \cong \frac{k_a C^{(110)} \phi_{Ti}^{(110)}}{k_i C^{(100)} \phi_{Ti}^{(100)}} \quad (4)$$

where $C^{(110)}$ and $C^{(100)}$ are the concentrations of sites available for Ti or donor coordination on the (110) and (100) MgCl$_2$ lateral cuts, respectively, and $\phi_{Ti}^{(110)}$ and $\phi_{Ti}^{(100)}$ are the fractions of these sites occupied by the Ti species.

On each kind of cut, if $\phi_{Ti}^{(1k0)} \ll \phi_D^{(1k0)}$ and hence $\phi_D^{(1k0)} \rightarrow 1$, that is for small adsorbed Ti fractions,

$$\phi_{Ti}^{(110)} \cong \frac{\phi_{Ti}^{(110)}}{\phi_D^{(110)}} = K^{(110)} \exp[-(E_{Ti}^{(110)} - E_D^{(110)})/RT] \quad (5)$$

$$\phi_{Ti}^{(100)} \cong \frac{\phi_{Ti}^{(100)}}{\phi_D^{(100)}} = K^{(100)} \exp[-(E_{Ti}^{(100)} - E_D^{(100)})/RT] \quad (6)$$

where $E_{Ti}^{(1k0)}$ and $E_D^{(1k0)}$ are coordination energies, and $\phi_{Ti}^{(1k0)}$ and $\phi_D^{(1k0)}$ are coverage fractions, with $\phi_{Ti}^{(1k0)} + \phi_D^{(1k0)} = 1$.

Taking for simplicity all other parameters constant but the coordination energies of the donors, $E_D^{(1k0)}$, eqs 5 and 6 can be simplified as follows:

$$\phi_{Ti}^{(110)} \cong K_1^{(110)} \exp(E_D^{(110)}/RT) \quad (7)$$

$$\phi_{Ti}^{(100)} \cong K_1^{(100)} \exp(E_D^{(100)}/RT) \quad (8)$$

where $K_1^{(1k0)} = K^{(1k0)} \exp(-E_{Ti}^{(1k0)}/RT)$. Combining eqs 7 and 8, it can be written that

$$\frac{\phi_{Ti}^{(110)}}{\phi_{Ti}^{(100)}} = \frac{K_1^{(110)}}{K_1^{(100)}} \frac{\exp(E_D^{(110)}/RT)}{\exp(E_D^{(100)}/RT)} = K_2 \exp[(E_D^{(110)} - E_D^{(100)})/RT] \quad (9)$$

and insertingeq 9 in eq 4 it is obtained that

$$\frac{1 - \text{w.i.}}{\text{w.i.}} \cong \frac{k_a C^{(110)}}{k_i C^{(100)}} K_2 \exp[(E_D^{(110)} - E_D^{(100)})/RT] \quad (10)$$

and hence

$$-RT \ln\left(\frac{1 - \text{w.i.}}{\text{w.i.}}\right) \cong \text{const} + E_D^{(100)} - E_D^{(110)} \quad (11)$$

If we assume instead $\phi_{Ti}^{(100)} \rightarrow 1$ and $\phi_{Ti}^{(110)} \ll \phi_D^{(110)}$, in a similar way it can be derived that

$$-RT \ln\left(\frac{1 - \text{w.i.}}{\text{w.i.}}\right) \cong \text{const} - E_D^{(110)} \quad (12)$$

5. Conclusions

The MM and AM1 semiempirical methods have been used to investigate the adsorption of Lewis bases on lateral cut of MgCl$_2$.

In particular, the adsorption of several 1,3-diethers bearing different substituents in position 2 has been modeled on the (110) and (100) cuts of MgCl$_2$. For both calculation methods, all considered donors preferentially coordinate to the (110) cut due to the lower intramolecular (associated with the donor deformation suitable for coordination on each cut) as well as intermolecular (mainly electrostatic) energy contributions. For the considered donors the calculated energy difference relative to the minimum-energy coordinations on the two MgCl$_2$ lateral cuts (ΔE) presents a qualitative relationship with donor ability to increase the isospecific behavior of MgCl$_2$/TiCl$_4$ catalysts in propene polymerization (measured as weight fraction of polymer insoluble in xylene (w.i.)).

A simple model, which assumes that the xylene-insoluble and -soluble polypropylene fractions are obtained by polymerization on (100) and (110) cuts,

respectively, and that the donors coordination compete with Ti catalytic species formation, is able to rationalize in a more quantitative way industrially relevant dependence of isotactic indexes on the chemical structure of the 1,3-diether donor.

References and Notes

(1) Montedison, British Patent 1,286,867, 1968.
(2) Montedison German Patent 2,230,672, 1972.
(3) Montedison and Mitsui Petrochemical, German Patent, 2,643,143, 1977.
(4) Montedison EP, 45, 977, 1982.
(5) Noristi, L.; Barbè, P. C.; Baruzzi, G. *Macromol. Chem*. **1995**, *192*, 115.
(6) Kashiwa, N.; Kojoh, S. *Macromol. Symp*. **1995**, *89*, 27.
(7) (a) Busico, V.; Corradini, P.; De Martino, L.; Proto, A.; Savino, V.; Albizzati, E. *Makromol. Chem*. **1985**, *186*, 1279. (b) Busico, V.; Corradini, P.; De Martino, L.; Proto, A.; Albizzati, E. *Makromol. Chem*. **1986**, *187*, 1115.
(8) Kashiwa, N. In *Proceedings of the MMI International Symposium on "Transition Metal Catalyzed Polymerization: Unsolved Problems"*, Aug 17−21, 1981, Midland, MI; Part A, p 379.
(9) Keii, T.; Suzuki, E.; Tamura, M.; Doi, Y. In *Proceedings of the MMI International Symposium on "Transition Metal Catalyzed Polymerization: Unsolved Problems"*, Aug 17−21, 1981, Midland, MI; Part A, p 97.
(10) Pino, P.; Rotzinger, B.; Von Achenbach, E. *Makromol. Chem*. **1985**, *s13*, 185.
(11) (a) Albizzati, E.; Giannini, U.; Morini, G.; Smith, C. A.; Zeigler, R. *Ziegler Catalyst*; Fink, G., Mulhaupt, R., Brintzinger, H. H., Eds.; Springer-Verlag: Berlin, 1995; p 413. (b) Albizzati, E.; Giannini, U.; Morini, G.; Galimberti, M.; Barino, L.; Scordamaglia, R. *Makromol. Chem., Macromol. Symp*. **1995**, *89*, 73.
(12) Corradini, P.; Barone, V.; Fusco, R.; Guerra, G. *Gazz. Chim. Ital*. **1983**, *113*, 601.
(13) Giannini, U.; Giunchi, G.; Albizzati, E.; Barbè, P. C. "*Frontiers in Polymerization Catalysis and Polymer Synthesis*"; NATO Advanced Research Workshop, Feb 1−6, 1987.
(14) Corradini, P.; Guerra, G.; Barone, V.; Fusco, R. *Eur. Polym. J*. **1980**, *16*, 835.
(15) Chien, J. C. W.; Wu, J. C. *Polym. Sci., Polym. Chem*. **1982**, *20*, 2461.
(16) (a) Barino, L.; Scordamaglia, R. *Macromol. Theory Simul*. **1998**, *7*, 407. (b) Barino, L.; Scordamaglia, R. *Macromol. Symp*. **1995**, *89*, 111.
(17) Iiskola, E.; Pelkonen, A.; Kakkonen, H.; Pursiainen, J.; Pakkanen, T. *Makromol. Chem., Rapid Commun*. **1993**, *14*, 133.
(18) Barino, L.; Scordamaglia, R. *Macromol. Theory Simul*. **1998**, *7*, 399.
(19) Brooks, B. R.; Bruccoleri, R. E.; Olafson, B. D.; States, D. J.; Swaminathan, S.; Karplus, M. *J. Comput. Chem*. **1983**, *4*, 187.
(20) Rappè, A. K.; Casewit, C. J.; Colwell, K. S.; Goddard, W. A.; Skiff, W. M. *J. Am. Chem. Soc*. **1992**, *114*, 100.
(21) (a) Valle, G.; Baruzzi, G.; Paganetto, G.; Depaoli, G.; Zannetti, R.; Marigo, A. *Inorg. Chim. Acta* **1989**, *156*, 157. (b) Agron, P. A.; Busing, W. R. *Acta Crystallogr*. **1985**, *C41*, 8.
(22) Guerra, G.; Longo, P.; Cavallo, L.; Corradini, P.; Resconi, L. *J. Am. Chem. Soc*. **1997**, *119*, 4394.
(23) Stewart, J. J. P "Mopac 93.00 Manual", Fujitzu Limited, Tokyo, Japan, 1993.
(24) Dewar, M. J. S.; Zoebish, E. G.; Healy, E. F.; Stewart, J. J. P. *J. Am. Chem. Soc*. **1985**, *107*, 3902.
(25) Stewart, J. J. P. *J. Comput. Chem*. **1989**, *10*, 210.
(26) Hutter, M. C.; Reimers, J. R.; Hush, N. S. *J. Phys. Chem. B* **1998**, *102*, 8080.
(27) Baerends, E. J.; Ellis, D. E.; Ros, P. *Chem. Phys*. **1973**, *2*, 41.
(28) Snijders, J. G.; Vernooijs, P.; Baerends, E. J. *At. Nucl. Data Tables* **1981**, *26*, 483.
(29) Vosko, S. H.; Wilk, L.; Nusair, M. *Can. J. Phys*. **1980**, *58*, 1200.
(30) Becke, A. *Phys. Rev. A* **1988**, *38*, 3098.
(31) Perdew, J. P. *Phys. Rev. B* **1986**, *33*, 8822.
(32) Perdew, J. P. *Phys. Rev. B* **1986**, *34*, 7406.
(33) Morini, G., unpublished results.

MA990959A